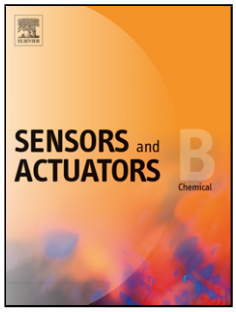

Title: Turn-On Fluorescence Sensor for Glutathione in Aqueous Solutions Using Carbon Dots-MnO_2 Nanocomposites

Author: Chunlei Yang Wenping Deng Haiyun Liu Shenguang Ge Mei Yan

PII: S0925-4005(15)00507-9
DOI: http://dx.doi.org/doi:10.1016/j.snb.2015.04.055
Reference: SNB 18360

To appear in: *Sensors and Actuators B*

Received date: 29-1-2015
Accepted date: 13-4-2015

Please cite this article as: C. Yang, W. Deng, H. Liu, S. Ge, M. Yan, Turn-On Fluorescence Sensor for Glutathione in Aqueous Solutions Using Carbon Dots-MnO_2 Nanocomposites, *Sensors and Actuators B: Chemical* (2015), http://dx.doi.org/10.1016/j.snb.2015.04.055

Turn-On Fluorescence Sensor for Glutathione in Aqueous Solutions Using Carbon Dots-MnO_2 Nanocomposites

Chunlei Yang[a], Wenping Deng[a], Haiyun Liu[a], Shenguang Ge[b], Mei Yan[a,*]

[a] Key Laboratory of Chemical Sensing & Analysis in Universities of Shandong, School of Chemistry and Chemical Engineering, University of Jinan, Jinan 250022, P. R. China

[b] Shandong Provincial Key Laboratory of Preparation and Measurement of Building Materials, University of Jinan, Jinan 250022, China

* Corresponding author: Mei Yan

E-mail: chm_yanm@126.com

Tel: +86-531-82767161

Fax: +86-531-88959988

Abstract: A novel fluorescence sensor based on carbon dots-MnO_2 nanocomposites was fabricated successfully, which can detect glutathione (GSH) in aqueous solutions succinctly, rapidly and selectively. The carbon dots (CDs), which were synthesized by using organosilane as a coordinating solvent, had a highly luminescent quantum yield. The nanoflower-like MnO_2 had an enormous specific surface area, which could react with more CDs. Subsequently, CDs-MnO_2 nanocomposites were synthesized through a facile one-step method. As a result of fluorescence resonance energy transfer (FRET) from CDs to the MnO_2, the fluorescence of CDs can be quenched by MnO_2. However, when GSH was introduced into the system, the quenched fluorescence could be restored because MnO_2 was reduced to Mn^{2+} by GSH, which led to the elimination of FRET. Compared with other electrolytes and biomolecules, we find that the chemical response of the CDs-MnO_2 nanocomposites exhibited good selectivity toward GSH. Under the optimal conditions, the proposed immunosensor was successfully performed with a linear range of 0.03 $\mu mol \cdot L^{-1}$ - 974.1 $\mu mol \cdot L^{-1}$, with a detection limit of 0.015 $\mu mol \cdot L^{-1}$. In addition, the proposed fluorescence sensor has several merits, such as low cost, good selectivity, great biocompatibility and chemical turn-on fluorescence response.

Keywords: carbon dots-MnO_2 nanocomposites; fluorescence; glutathione; fluorescence sensor

1. Introduction

Glutathione (γ-L-glutamyl-L-cysteinylglycine) is a special water-soluble peptide with the most prevalent low-molecular weight thiol in mammalian cells, which is synthesized endogenously from the precursor amino acids L-cysteine, L-glutamic acid, and glycine [1,2]. Under normal circumstances, this tripeptide can be found in oxidized disulfide (GSSG) or reduced thiol (GSH) states and the major existing form is the reduced form (GSH). Glutathione is used in vivo almost exclusively in the reduced state hence the importance of a high GSH/GSSG ratio in the cell can never be ignored [3]. Recent studies have demonstrated that GSH have played a more and more important role in a variety of molecular reactions and biological applications in many cellular processes, including amino acid transportation, detoxification of xenobiotics, maintenance of protein redox state, neuromodulation and neurotransmission [4]. What's more, the level of GSH in tissues is related to a variety of diseases, such as AIDS, Alzheimer disease, alcoholic liver disease, cardiovascular disease, diabetes mellitus, and cancer [5-10]. Because of the biological importance of GSH, there are numbers of approaches to quantify or monitor the changes of GSH in samples, including high-performance liquid chromatography [11], electrochemistry [12], electrogenerated chemiluminescence [13], surface-enhanced raman scattering [14], mass spectrometry [15] and fluorescence spectroscopy [16]. Compared with other analytical methods, fluorescence spectroscopy has significant advantages for its high sensitivity, simplicity, and nondestructive properties [17]. Therefore, we adopt the method of fluorescence spectroscopy for the GSH detection, which may be a valuable

research.

Fluorescent probes have been recognized as the most efficient molecular tools that can help monitor and visualize trace amounts of samples in live cells or tissues because of its high sensitivity and high spatiotemporal resolution [18]. Nowadays, a variety of materials, such as organic fluorophores [19], gold nanoclusters [20], quantum dots (QDs) [21] and carbon nanomaterials [22] have been used as fluorescent probes. Among them，QDs have become one of the most extensively optical sensing nanomaterials in the detection of nucleic acids, enzymes, proteins, metal ions, and other small molecules because of high emission quantum yields and size tunable emission profiles [23]. However, those popular QDs have serious toxicity even at relatively low concentration [24]. In contrast with common QDs, carbon dots (CDs) have no burden of intrinsic toxicity or elemental scarcity and do not need for stringent, intricate, tedious, costly, or inefficient preparation steps. Therefore, CDs have attracted much interest in various fields, such as biosensing and bioimaging in live cells. At the same time because of their excellent luminescence properties, CDs have been used as benign fluorescent probes [25,26]. Hence, a design of a fluorescent probe for detecting GSH based on CDs could be available.

Manganese oxide nanoparticles have high reactivity, specificity and can be used as both catalyst and reactant. Among them, manganese dioxide (MnO_2) is one of the most stable manganese oxides with excellent physical and chemical properties under ambient conditions [27-30]. As a type of transition metal oxide, it has drawn an increasing amount of attention in batteries, supercapacitors and even visible

light-driven catalysis [31-34]. However, it has rarely been reported in fluorescence strategy [35]. A special morphological MnO_2 is of great interest because of their unique properties including exceptionally high specific surface area and unique electronic property. Among them, MnO_2 nanoparticles have a broad absorption spectrum (250-550 nm) [36]. The spectrum overlaps with the fluorescence excitation and/or emission spectra of most kinds of fluorescent dyes. This feature allows the occurrence of FRET [37] with MnO_2 nanomaterials, of which the FRET mechanism has recently been utilized for fluorescent sensing [38]. In our work, we synthesized a nanoflower-like MnO_2 which have an enormous specific surface area by a microemulsion method. The novel materials have the merits of nanoparticles, and at the same time have controllable particle size, nice particle dispersion and narrow size distribution, which have a broad application prospect. Thus, the prepared nanoflower-like MnO_2 was applied to fluorescence strategy in our work.

In this paper, a turn-on fluorescence sensor for GSH in aqueous solutions was fabricated successfully. We first used a delicate one-step method to produce CDs-MnO_2 nanocomposites which was used for detecting GSH rapidly and selectively in aqueous solution. The sensor we established exhibits superior selectivity for GSH chemical response parallel with other biomolecules and electrolytes, which may be promising to apply for monitoring changes of the intracellular GSH level in living cells. The nanoflower-like MnO_2 nanoparticles we prepared exhibit an enormous specific surface area, hence, may combine much more CDs. The CDs are low-toxicity and eco-friendly, which have highly luminescence, benign optical

properties and inherent stability. They have drawn increasing attention owing to their biocompatible and nontoxic characters, demonstrating attractive applications in biosensor and biomedical imaging. As a result of FRET from CDs to the MnO_2, the formed CDs-MnO_2 nanocomposites can quench the fluorescence of CDs. When GSH appeared the system, the quenched fluorescence would be restored, which could be the reason that GSH reduced the MnO_2 to Mn^{2+}.As far as we know, the CDs-MnO_2 nanocomposites fluorescence sensor could be demonstrated firstly for GSH detection and its application to constitute a fluorescent method for in vivo sensing of GSH may be promising.

2. Experimental section

2. 1. Chemicals and materials

N-(β-aminoethyl)-γ-aminopropyl methyldimethoxy silane (AEAPMS) was purchased from Beijing Shenda Fine Chemical Co, Ltd.(Beijing, China). Citric acid anhydrous and potassium hypermanganate ($KMnO_4$) were purchased from Shanghai Chemical Reagent Company (Shanghai, China). Oleic acid was purchased from sinopharm chemical Reagent Co., Ltd. 3-Aminopropyltrimethoxysilane (APTS) and ethyl dimethyamino cabodiimide hydrochloride (EDC·HCl) were purchased from Xiya Reagent Research Center No.67 Chang Lin Rd, Linshu, Shandong. Rabbit liver metallothionein (MT) II was purchased from Shanghai Sangon Biotechnology Co., Ltd. (China). Glycine (Gly), D-aspartic acid (Asp), thioredoxin (Trx) (from Escherichia coli), glucose, bovine serum albumin (BSA), GSH (reduced form), glutathione reductase (GR) and other reagents of analytical reagent grade were

purchased from Aladdin Co., Ltd (Shanghai, China). All reagents were of analytical grade reagent or the highest purity available and directly used for the following experiments without further purification and the aqueous solutions unless indicated were prepared with doubly distilled water.

2. 2. Apparatus

The morphology and composition of the prepared materials were characterized by a QUANTA FEG 250 thermal field emission scanning electron microscope (SEM, FEI Co., USA) and energy dispersive X-ray spectroscopy (EDS) equipped with an X-MAX50 X-ray energy dispersive spectrometer (Oxford Co., UK), operated at 15 kV. Ultraviolet-visible light (UV-vis) absorption spectra were recorded on a UV-2550 spectrophotometer (Shimadzu Suzhou instruments Mfg. Co. Ltd.) in the range of 200-800 nm. Fluorescence spectra were collected using a RF-5301PC fluorophotometer (Shimadzu Co., Ltd., Japan). The samples were excited at 325 nm and the fluorescence emission ranged from 360 nm to 600 nm, in steps of 1 nm. All UV-vis absorption and fluorescence measurements were measured at room temperature.

2. 3. The synthesis of CDs

CDs were synthensized according to previous typical literature [39]. Firstly, 10 mL AEAPMS were placed into a 100 mL three-necked flask, and degassed with nitrogen for 5 min. After that, the flask was heated and till 240 °C, 0.5 g citric acid anhydrous was then quickly added to the solution with vigorous stirring. The mixture was then kept at the temperature for 1 min. Finally, the final products were purified by

precipitation with petroleum ether for three times; about 2 mL CDs were obtained.

2. 4. Preparation of MnO_2 nanoflowers

MnO_2 Nanoflowers were prepared by a typical procedure [40]. In brief, 0.2500 g $KMnO_4$ was dissolved in 125 mL of ultrapure water, and the mixture was stirred for about 0.5 h. Subsequently, 2.5 mL of oleic acid was then added, and a steady emulsion was formed. After the emulsion was maintained at room temperature for 24 h, a brown-black product was collected, and washed several times with ultrapure water and alcohol to remove any possible residual reactants. Finally, the product was dried in air at 60 °C for 12 h.

2. 5. The synthesis of CDs-MnO_2 nanocomposites

The MnO_2 nanoflowers were first reacted with aminopropyltrimethoxysilane (APTS) to modify their surface with NH_2 groups [41]. Typically, MnO_2 nanoflowers (50 mg), APTS (100 μL), and toluene (16 mL) were added successively into a 250 mL round-bottomed flask. Afterwards, the reaction mixture was stirred and refluxed at 120 ℃ under N_2 for 6 h. The modified MnO_2 nanoflowers were then washed with toluene, and dried in air at 60 ℃. 1 mg modified MnO_2 nanoflowers were firstly dissolved in 10 mL ultrapure water by sonication. In a typical reaction, 200 μL CDs solution was added to 2.5 mL PBS buffer (0.1 M, pH 7.0). 500 μL of MnO_2 solution and 3 mg EDC·HCl were then added and the volume of mixture was adjusted to 10 mL with ultrapure water. After that, the resulting mixture was sonicated for 30 min so that the reaction could be completely finished.

2. 6. Fluorescence sensing of GSH

The sensing solutions were prepared by mixing 100 μL of CDs-MnO_2 nanocomposites solutions with 100 μL of GSH with different concentrations in 1.5 mL centrifuge tubes at room temperature. The solutions were then diluted in 1 mL in ultrapure water and mixed thoroughly in different incubation reaction time. Afterward, the fluorescence emission spectra of the mixtures were recorded with excitation at 325 nm and the fluorescence intensity of CDs-MnO_2 nanocomposites by GSH in different incubation time was studied.

3. Results and discussion

3. 1. Possible mechanism for the sensor

Figure 1 demonstrated the principle of CDs-MnO_2 nanocomposites sensor for GSH. The MnO_2 nanoflowers with functionalized amino groups could be easily connected with CDs via an acylation process, which had active group carboxyl on the surface. Similarly, the -NH_2 modified MnO_2 nanoflowers would react with CDs that were modified with -COOH. Thus, the CDs-MnO_2 nanocomposites could be easily obtained and the nanocomposites are very stable. When GSH is injected into the system, MnO_2 could be reduced by GSH, which lead to the inhibition of the FRET process between CDs and MnO_2, so the fluorescence intensity restores. In the redox process, MnO_2 was reduced to Mn^{2+} and GSH (via the sulfhydryl groups [−SH]) was oxidized to glutathione disulfide (GSSG) via -SH exchange [36], as shown by the equation below.

$$MnO_2+2GSH+2H^+ \rightarrow Mn^{2+}+GSSG+2H_2O$$

Hence, the simple and facile CDs-MnO_2 nanocomposites could be as a fluorescence

sensor for rapid screening and quantification of the GSH levels.

Scheme 1

3. 2. The characterization of CDs, MnO_2 and CDs-MnO_2 nanocomposites

Optical properties of the CDs were characterized by UV-vis absorption and fluorescence spectroscopy. As shown in Figure 1A (a), CDs have an obvious moderate UV absorption at 200 nm-400 nm. Furthermore, an absorption edge extending to 400 nm was only found in CDs, indicating the formation of CDs [42]. Under the excitation of 325 nm, the CDs exhibit distinct fluorescence emission at 458 nm (Figure 1A (b)). The inset in Figure 1A is the photographs of diluted solutions of CDs, which is nearly colorless (or a very slight yellow color) under visible light, while it emits intense green fluorescence under a 365 nm UV light. Figure 1B displays the fluorescence spectroscopy of CDs solutions and the UV-vis absorption spectrum of MnO_2 nanoparticles which was synthesized by microemulsion method. It can be observed that MnO_2 nanoparticles (Figure 1B (a)) have a broad absorption band from 250 nm to 550 nm, which matches well with the previous reported optical characteristic of MnO_2 nanomaterials [36, 43].Obviously, as shown in Figure 1B, the absorbance spectrum of MnO_2 nanoparticles overlaps well with the fluorescence emission of the CDs, which leads to FRET from the CDs to the MnO_2. To get a further understanding of the morphology of MnO_2 nanoparticles, the TEM image is displayed in Figure 1C. As seen from the TEM image, the MnO_2 nanoparticles of 200 nm in diameter have a nanoflower-like structure that formed by the self-assembly of MnO_2 nanoplatelets. A typical energy-dispersive spectrometry (EDS) spectrum of MnO_2 products is shown in

Figure 1D, which shows that the obtained deposits are pure MnO_2.

Figure 1

The formation of CDs-MnO_2 nanocomposites is characterized by UV-vis absorption spectrum and fluorescence spectrum. A broad absorption peak at 400 nm was displayed in Figure 2A (b), which demonstrates the characteristic of MnO_2 nanomaterials. In addition, the fluorescence spectrum of CDs-MnO_2 nanocomposites in Figure 2B (b) further testify the formation of CDs-MnO_2, which have an apparent extinction of fluorescence intensity than CDs. Figure 2C demonstrates the fluorescence response of CDs modified with different concentrations of MnO_2 (from 0 mM to 0.04 mM). As expected, the fluorescence intensity of CDs decreased as the MnO_2 concentration increased (Figure 2C). A good liner relationship is observed in Figure 2D. The fitted equation is Y=-1.48781+5054.58484X with the concentration of MnO_2 in the range of 0-0.04 mM (R^2 = 0.9968), as displayed in Figure 2D. This is possibly because the MnO_2 had larger superficial area, with the MnO_2 concentration increasing, the absorption capacity to CDs became higher, which lead to the fluorescence of CDs be more heavily quenched.

Figure 2

3. 3. Fluorescence sensing of GSH based on the CDs-MnO_2 nanocomposites

The kinetics of the reaction between GSH and CDs-MnO_2 nanocomposites was measured in a spectrofluorometer by monitoring the fluorescence recovery on the basis of time. Figure 3A shows that the fluorescence intensity of CDs gradually increases with the reaction time. The whole approach reached equilibrium at about 3

min, which displays a rapid react process at room temperature. We select 3 min as incubation time for sensitive measurement of GSH in the subsequent experiment.

Figure 3

We researched the fluorescence response of CDs-MnO_2 nanocomposites after incubation 3 min with different GSH concentrations in aqueous solutions for the purpose of studying the applicability of the fluorescence sensor for GSH determination. With the increase of GSH concentration from 0 mM to 2 mM, the fluorescence of the CDs restored gradually and the sensing response reached the maximum finally, which showed no further more fluorescent enhancement. The inset in Figure 3B shows the plot of fluorescence enhancement ($F-F_0$) against the concentration of GSH The equation of fitted curve is Y=171.3-242.8/(1+exp((X-316.3)/432.9)). The fitted curve could be used for the quantification of GSH with a correlation coefficient of 0.9975, and the detection limit could reach as low as 0.015 μM based on the definition of 3 times the deviation of the blank signal (3σ).The liner fitted equation is Y=9.08669+0.12413X, R^2=0.9957. We attain the final result that the linear range is 0.03 $\mu mol \cdot L^{-1}$-974.1 $\mu mol \cdot L^{-1}$ by calculation.

3. 4. Selectivity of CDs-MnO_2 nanocomposites based turn-on fluorescence sensor toward GSH

Selectivity is a critical parameter to evaluate the performance of a fluorescence immunosensor. The influence of some electrolytes and biomolecules (amino acids, proteins, etc.) was added into aqueous solutions to evaluate the selectivity of

CDs-MnO_2 nanocomposites for GSH and the experimental results was shown in Figure 4. Figure 4A demonstrates that CDs-MnO_2 nanocomposites exhibit a higher fluorescence response toward GSH concentrations from 200 μM to 500 μM. However, we don't observe a noticeable fluorescence response changes with other electrolytes and biomolecules. In addition, protein thiols at the intracellular or higher concentration [44] produced a very low fluorescence response, which could be owing to the steric factor between nanocomposites and protein (including GR, Trx, MT in Figure 4A). What's more, some nonthiol reducing agents (Vitamin E, Vitamin C, NADPH, NADH in Figure 4B) at the concentrations according to the intracellular concentrations or slightly more than intracellular concentrations [44, 45] was also detected. The experimental results are shown in Figure 4B. On the average, the Figure 4 shows that CDs-MnO_2 nanocomposites display a highly selective fluorescence response toward GSH over other nontarget samples.

Figure 4

4. Conclusions

In this study, a simple and efficient CDs-MnO_2 nanocomposites were prepared by a facile one-step acylation process route combined with a mild ultrasonic method. Because of FRET from CDs to the MnO_2, the fluorescence of the formed CDs can be quenched by MnO_2. When GSH was introduced into the system, the quenched fluorescence could be restored. Therefore, this fluorescence turn-on nanoprobe has been successfully applied to monitor changes of the GSH level in solution and is promising to be applied to monitor intracellular GSH level in living cells. Compared

with other electrolytes and biomolecules, the chemical response of the CDs-MnO_2 nanocomposites exhibits good selectivity toward GSH. In the meanwhile, the CDs-MnO_2 nanocomposites have several appealing features, including low cost, easy preparation, low biotoxicity, nice biocompatibility and turn-on fluorescence response. As a result, the immunoassay exhibited high sensitivity, excellent selectivity, low detection limit and accepted precision on the detection of GSH. Therefore, the novel fluorescence sensor may have a promising applicability for quantitative GSH detection.

Acknowledgements

This work was financially supported by National Natural Science Foundation of China (51273084, 51473067, 21277058), Natural Science Foundation of Shandong Province, China (ZR2012BZ002), Technology Development Plan of Shandong Province, China (Grant No.2012GGB01181).

References

[1] T. M. Bray, C. G. Taylor, Tissue glutathione, nutrition, and oxidative stress, Canadian Journal of Physiology and Pharmacology 71 (1993) 746 - 751.

[2] A. Meister, M. E. Anderson, glutathione, Annual Review of Biochemistry 52 (1983) 711 - 760.

[3] W. Droge, Free radicals in the physiological control of cell function, Physiological Reviews 82 (2002) 47 - 95.

[4] A. Paolicchi, S. Dominici, L. Pieri, E. Maellaro, A. Pompella, Glutathione catabolism as a signaling mechanism, Biochemical Pharmacology 64 (2002) 1027 - 1035.

[5] A. Pastore, G. Federici, E. Bertini, F. Piemonte, Analysis of glutathione: implication in redox and detoxification, Clinica Chimica Acta 333 (2003) 19 - 39.

[6] J. Navarro, E. Obrador, J. Carretero, I. Petschen; J. Avino, P. Perez, J. M. Estrela, Changes in glutathione status and the antioxidant system in blood and in cancer cells associate with tumour growth in vivo, Free Radical Biology and Medicine 26 (1999) 410 - 418.

[7] D. M. Townsend, V. J. Findlay, F. Fazilev, M. Ogle, J. Fraser, J. E. Saavedra, X. Ji, L. K. Keefer, K. D. Tew, A glutathione S-transferase π activated pro-drug causes kinase activation concurrent with S-glutathionylation of proteins, Molecular Pharmacology 69 (2006) 501 - 508.

[8] J. M. Estrela, A. Ortega, E. Obrador, Glutathione in cancer biology and therapy,

Critical Reviews in Clinical Laboratory Sciences 43 (2006) 143 - 181.

[9] M. Kemp, Y. M. Go, D. P. Jones, Nonequilibrium thermodynamics of thiol/disulfide redox systems: a perspective on redox systems biology, Free Radical Biology and Medicine 44 (2008) 921 - 937.

[10] C. Perricone, C. De Carolis, R. Perricone, Glutathione: a key player in autoimmunity, Autoimmunity Reviews 8 (2009) 697 - 701.

[11] D. J. Reed, J. R. Babson, P. W. Beatty, A. E. Brodie, W.W. Ellis, D. W. Potter, High-performance liquid chromatography analysis of nanomole levels of glutathione, glutathione disulfide, and related thiols and disulfides, Analytical Biochemistry 106 (1980) 55 - 62.

[12] A. Safavi, N. Maleki, E. Farjami, F. A. Mahyari, Simultaneous Electrochemical Determination of Glutathione and Glutathione Disulfide at a Nanoscale Copper Hydroxide Composite Carbon Ionic Liquid Electrode, Analytical Chemistry 81 (2009) 7538 - 7543.

[13] Y. Wang, J. Lu, L. Tang, H. Chang, J. Li, Graphene Oxide Amplified Electrogenerated Chemiluminescence of Quantum Dots and Its Selective Sensing for Glutathione from Thiol-Containing Compounds, Analytical Chemistry 81 (2009) 9710 - 9715.

[14] A. Saha, N. R. Jana, Detection of Cellular Glutathione and Oxidized Glutathione using Magnetic-Plasmonic Nanocomposite based “Turn-Off” Surface Enhanced Raman Scattering, Analytical Chemistry 85 (2013) 9221 - 9228.

[15] X. Zhu, N. Kalyanaraman, R. Subramanian, Enhanced screening of glutathione

trapped reactive metabolites by in-source collision-induced dissociation and extraction of product ion using UHPLC-high resolution mass spectrometry, Analytical Chemistry 83 (2011) 9516 - 9523.

[16] R. Huang, X. Wang, D. Wang, F. Liu, B. Mei, A. Tang, J. Jiang, G. Liang, Multifunctional Fluorescent Probe for Sequential Detections of Glutathione and Caspase-3 in Vitro and in Cells, Analytical Chemistry 85 (2013) 6203 - 6207.

[17] Y. Yang, Q. Zhao, W. Feng, F. Li, Luminescent chemodosimeters for bioimaging, Chemical Reviews 113 (2013) 192 - 270.

[18] T. Ueno, T. Nagano, Fluorescent probes for sensing and imaging, Nature Methods 8 (2011) 642 - 645.

[19] N. Shao, J. Jin, H. Wang, J.Zheng, R. Yang, W. Chan, A. Zeper, Design of Bis-spiropyran Ligands as Dipolar Molecule Receptors and Application to in Vivo Glutathione Fluorescent Probes, Journal of the American Chemical Society 132 (2010) 725 - 736.

[20] D. Tian, Z. Qian, Y. Xia, C. Zhu, Gold nanocluster-based fluorescent probes for near-infrared and turning-on sensing of glutathione in living cells, Langmuir 28 (2012) 3945 - 3951.

[21] J. Liu, C. Bao, X. Zhong, C. Zhao, L. Zhu, Highly Selective Detection of Glutathione Using Quantum-Dots-Based OFF-ON Fluorescent Probes, Chemical Communications 46 (2010) 2971 - 2973.

[22] L. Zhou, Y. Lin, Z. Huang, J. Ren, X. Qu, Carbon nanodots as fluorescence probes for rapid, sensitive, and label-free detection of Hg^{2+} and biothiols in

353 complex matrices, Chemical Communications 48 (2012) 1147 - 1149.

354 [23] X. Xu, X. Liu, Z. Nie, Y. Pan, M. Guo, S. Yao, Label-Free Fluorescent Detection
355 of Protein Kinase Activity Based on the Aggregation Behavior of Unmodified
356 Quantum Dots, Analytical Chemistry 83 (2011) 52 - 59.

357 [24] A. M. Derfus, W. C. W. Chan, S. N. Bhatia, Probing the cytotoxicity of
358 semiconductor quantum dots, Nano Letters 4 (2004) 11-18.

359 [25] Y. P .Sun, B. Zhou, Y. Lin, W. Wang, K. A. S. Fernando, P. Pathak, M. J. Meziani,
360 B. A. Harruff, X. Wang, H. F. Wang, P. G. Luo, H. Yang, M. E. Kose, B. L. Chen,
361 L. M. Veca, S. Y .Xie, Quantum-Sized Carbon Dots for Bright and Colorful
362 Photoluminescence, Journal of the American Chemical Society 128 (2006) 7756
363 - 7757.

364 [26] S. N. Baker, G. A. Baker, Luminescent Carbon Nanodots: Emergent Nanolights,
365 Angewandte Chemie International Edition 49 (2010) 6726 - 6744.

366 [27] T. A. Zordan, L. G. Hepler, Thermochemistry and oxidation potentials of
367 manganese and its compounds, Chemical Reviews 68 (1968) 737 - 745.

368 [28] H. Zhang, G. Cao, Z. Wang, Y. Yang, Z. Shi, Z. Gu, Growth of Manganese Oxide
369 Nanoflowers on Vertically-Aligned Carbon Nanotube Arrays for High-Rate
370 Electrochemical Capacitive Energy Storage, Nano Letters 8 (2008) 2664 - 2668.

371 [29] F. Cheng, J. Zhao, W. Song, C. Li, H. Ma, J. Chen, P. Shen, Facile controlled
372 synthesis of MnO_2 nanostructures of novel shapes and their application in
373 batteries, Inorganic Chemistry 45 (2006) 2038 - 2044.

374 [30] V. Subramanian, H. Zhu, B. Wei, Alcohol-assisted room temperature synthesis of

different nanostructured manganese oxides and their pseudocapacitance properties in neutral electrolyte, Chemical Physics Letters 453 (2008) 242 - 249.

[31] D. Liu, B. B. Garcia, Q. Zhang, Q. Guo, Y. Zhang, S. Sepehri, G. Cao, Mesoporous Hydrous Manganese Dioxide Nanowall Arrays with Large Lithium Ion Energy Storage Capacities, Advanced Functional Materials 19 (2009) 1015 - 1023.

[32] W. Wei, X. Cui, W. Chen, D. G. Ivey, Manganese oxide-based materials as electrochemical supercapacitor electrodes, Chemical Society Reviews 40 (2011) 1697 - 1721.

[33] R. Brimblecombe, A. Koo, G. C. Dismukes, G. F. Swiegers, L. Spiccia, Solar Driven Water Oxidation by a Bioinspired Manganese Molecular Catalyst, Journal of the American Chemical Society 132 (2010) 2892 - 2894.

[34] V. B. R. Boppana, S. Yusuf, G. S. Hutchings, F. Jiao, Nanostructured Alkaline-Cation-Containing δ-MnO_2 for Photocatalytic Water Oxidation, Advanced Functional Materials 23 (2013) 878 - 884.

[35] W. Y. Zhai, C. X. Wang, P. Yu, Y. X. Wang, L. Q. Mao, Single-Layer MnO2 Nanosheets Suppressed Fluorescence of 7-Hydroxycoumarin: Mechanistic Study and Application for Sensitive Sensing of Ascorbic Acid in Vivo, Analytical Chemistry 86 (2014) 12206 - 12213.

[36] R. Deng, X. Xie, M. Vendrell, Y. T. Chang, X. Liu, Intracellular glutathione detection using MnO_2-nanosheet modified upconversion nanoparticles, Journal of the American Chemical Society 133 (2011) 20168 - 20171.

[37] J. R. Lakowicz, Principles of Fluorescence Spectroscopy, 2nd ed. Kluwer Academic/Plenum Publishers, New York (1999) 698.

[38] H. Dong, W. Gao, F. Yan, H. Ji, H. Ju, Fluorescence resonance energy transfer between quantum dots and graphene oxide for sensing biomolecules, Analytical Chemistry 82 (2010) 5511 - 5517.

[39] F. Wang, Z. Xie, H. Zhang, C. Y. Liu, Y. G. Zhang, Highly Luminescent Organosilane-Functionalized Carbon Dots, Advanced Functional Materials 21 (2011) 1027 - 1031.

[40] J. Y. Zhu, J. H. He, Facile Synthesis of Graphene-Wrapped Honeycomb MnO_2 Nanospheres and Their Application in Supercapacitors, Applied Materials & Interfaces 4 (2012) 1770 - 1776.

[41] S. Yang, X. Feng, S. Ivanovici, K. Müllen, Fabrication of graphene-encapsulated oxide nanoparticles: towards high-performance anode materials for lithium storage, Angewandte Chemie International Edition 49 (2010) 8408 - 8411.

[42] A. Jaiswal, S. S. Ghosh, A. Chattopadhyay, One step synthesis of C-dots by microwave mediated caramelization of poly(ethylene glycol), Chemical Communications 48 (2012) 407 - 409.

[43] G. Zhao, J. Li, L. Jiang, H. Dong, X. Wang, W. Hu, Synthesizing MnO_2 nanosheets from graphene oxide templates for high performance pseudosupercapacitors, Chemical Science 3 (2012) 433 - 437.

[44] B. Tang, Y. Xing, P. Li, N. Zhang, F. Yu, G. Yang, A rhodamine-based fluorescent probe containing a Se-N bond for detecting thiols and its application in living

419 cells, Journal of the American Chemical Society 129 (2007) 11666 - 11667.

420 [45] Y. P. Hung, J. G. Albeck, M. Tantama, G. Yellen, Imaging cytosolic NADH-NAD^+

421 redox state with a genetically encoded fluorescent biosensor, Cell Metabolism 14

422 (2011) 545 - 554.

423

Biographies

Chunlei Yang studies in school of chemistry and chemical engineering, University of Jinan as postgraduate student.

Wenping Deng studies in school of chemistry and chemical engineering, University of Jinan as postgraduate student.

Haiyun Liu received his PhD degree in Chemical Engineering and Materials Science from Shandong Normal University in 2014. He then worked in University of Jinan, where currently he is a lecturer of chemistry. His current scientific interests are focused on nucleic acid DNA-based sensor, bio-imaging and biochemical analysis.

Shenguang Ge received his PhD degree in Chemistry and Chemical Engineering in 2013 from Shandong University, completed his master degree studies in University of Jinan in 2006. He joined University of Jinan, where currently he is a lecturer of chemistry. His research interests are in the area of biosensor and chemsensor.

Mei Yan received her BSc in applied chemistry from University of Jinan in 1999, and obtained her PhD in 2005 from Institute of chemistry Chinese Academy of Sciences. She then joined University of Jinan, as an associate professor working on the synthesis and performance of advanced functional materials.

Figure Captions

Scheme 1. Schematic representation of CDs-MnO_2 nanocomposites for sensing of GSH.

Figure 1. (A) UV-vis absorption (a) and fluorescence spectra (b) of CDs solution. Inset shows the color change of CDs solution without and with UV irradiation. (B) Spectral overlap showing the UV-vis absorption spectrum of MnO_2 nanoparticles (a) and the fluorescence emission spectrum of the CDs (b).(C) Representative TEM images of nanoflower-like MnO_2 nanoparticles. (D)EDS of MnO_2 nanoparticles.

Figure 2. (A) UV-vis absorption spectra of the CDs (a) and CDs-MnO_2 nanocomposites (b). (B) Fluorescence spectra of CDs (a) and CDs-MnO_2 nanocomposites (b). (C) Fluorescence spectra of CDs-MnO_2 prepared by different concentrations of MnO_2 (a, b, c, d, e, f, g, h represent 0, 0.0051, 0.0102, 0.0153, 0.0204, 0.0256, 0.0307, 0.0358 mM respectively.) at excitation wavelength of 400 nm. (D) The liner relationship of MnO_2 concentration and nanocomposite fluorescence intensity.

Figure 3. (A) Fluorescence response of CDs-MnO_2 nanocomposites in the presence of GSH (1 mM) (a) and in the absence of GSH (b), as a function of time. (B) Fluorescence emission spectra of CDs-MnO_2 nanocomposites in the presence of different concentrations of GSH (0-2 mM). The inset shows plot of the fluorescence intensity versus GSH concentration (0-2 mM).

Figure 4. Fluorescence response of the CDs-MnO_2 nanocomposites toward (A) GSH, different electrolytes and biomolecules (B) NADPH, NADH ,Vitamin C, Vitamin E,

462 (50 μM for each) and GSH. F and F_0 represent the fluorescence intensity in the
463 presence of the target (GSH) and the response of water, respectively.

Graphical Abstract (for review)

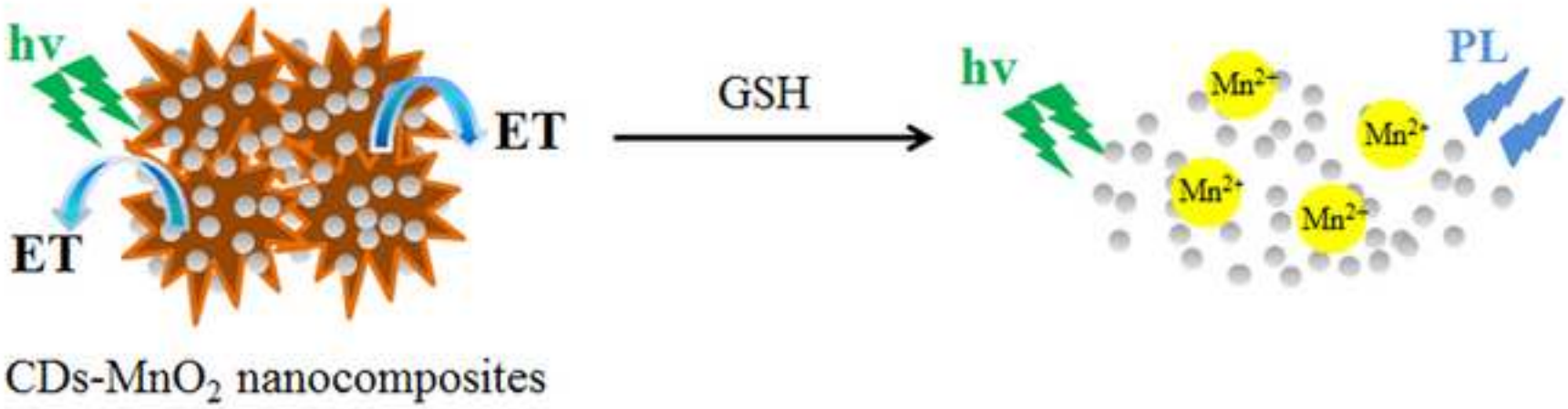

Scheme 1

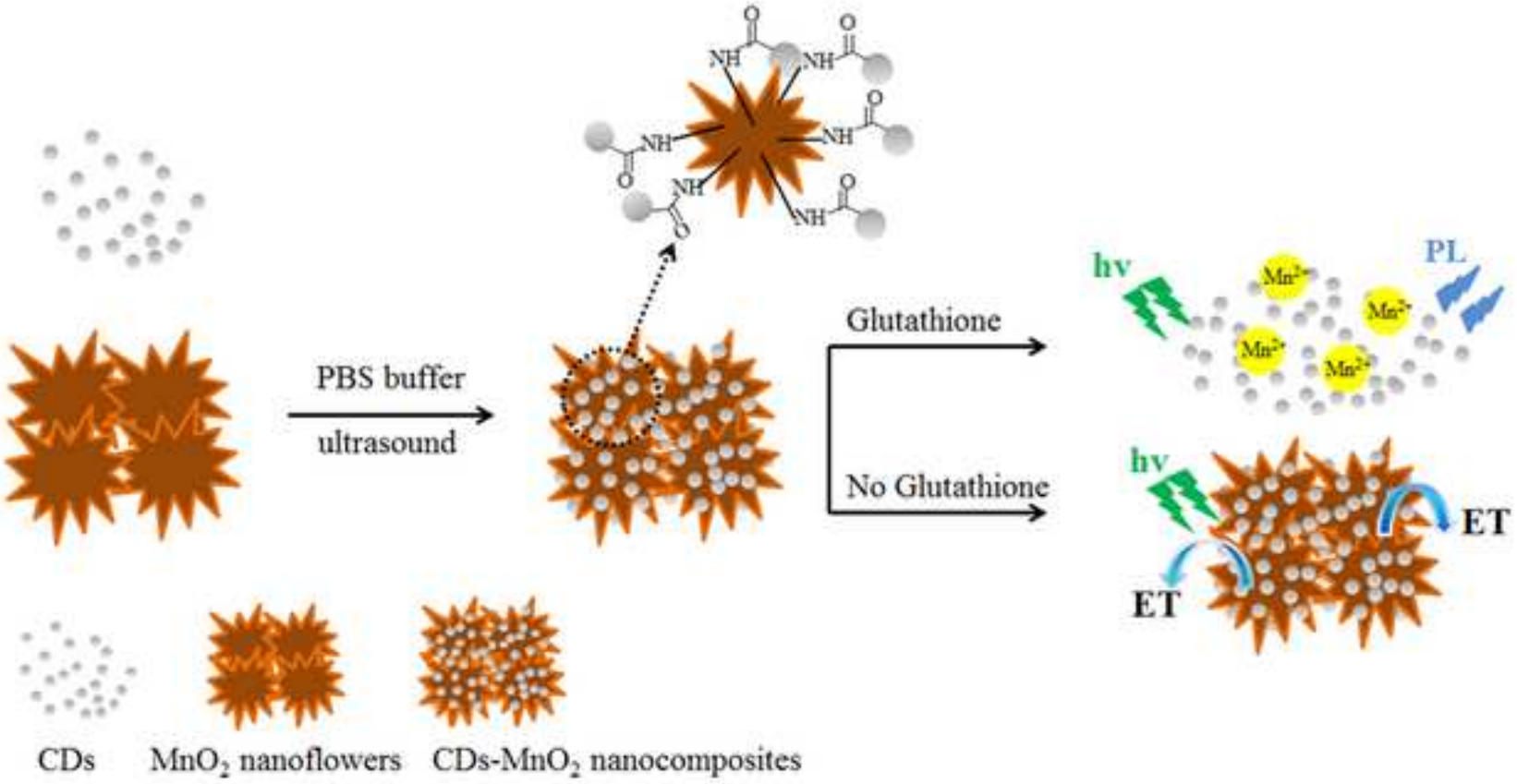
PBS buffer
ultrasound
Glutathione
No Glutathione
hv
PL
ET
ET
CDs
MnO2 nanoflowers
CDs-MnO2 nanocomposites

Figure 1

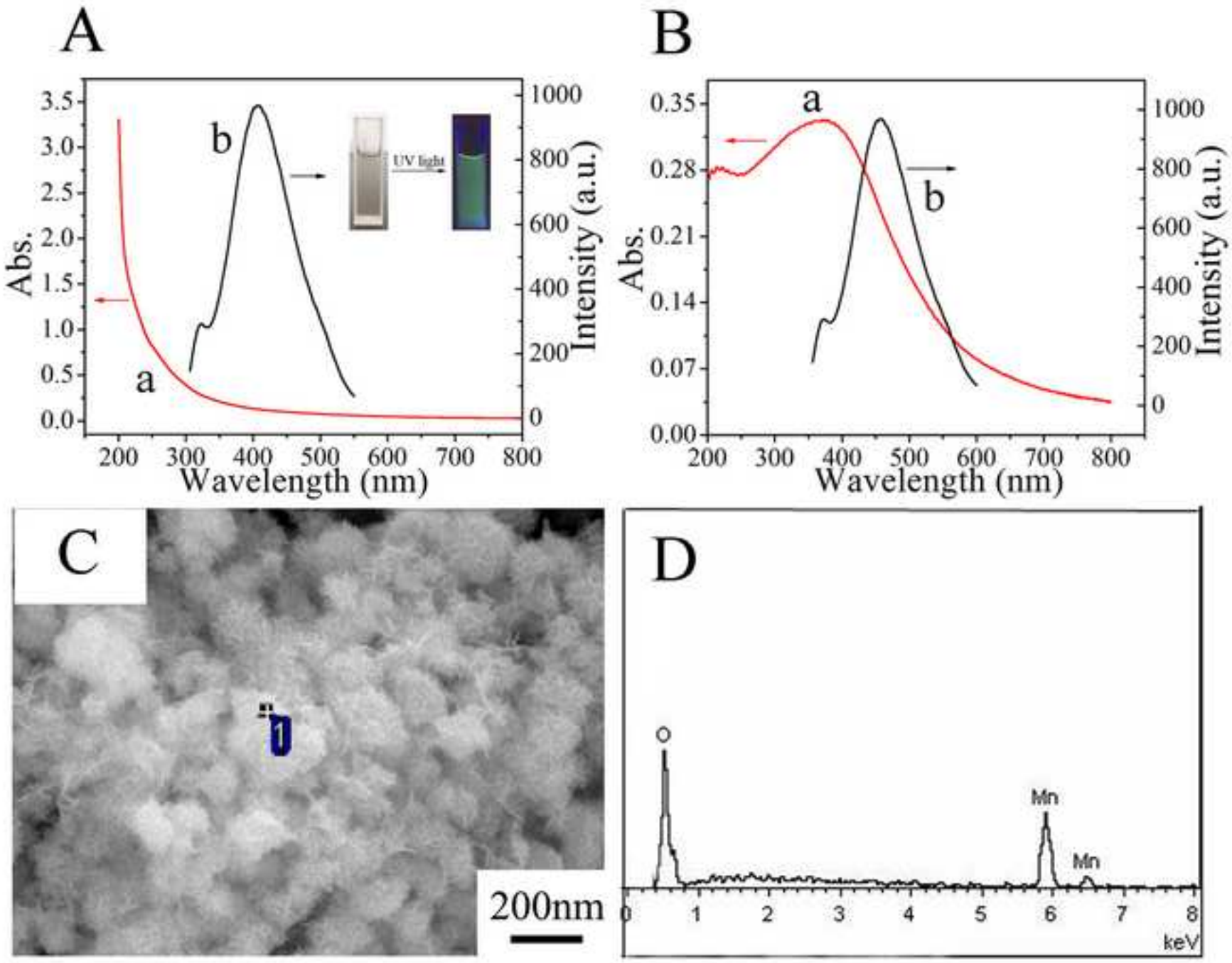
A
B
C
D
Abs.
Intensity (a.u.)
Wavelength (nm)
a
b
UV light
200nm
Mn
Mn
O
keV

Figure 2

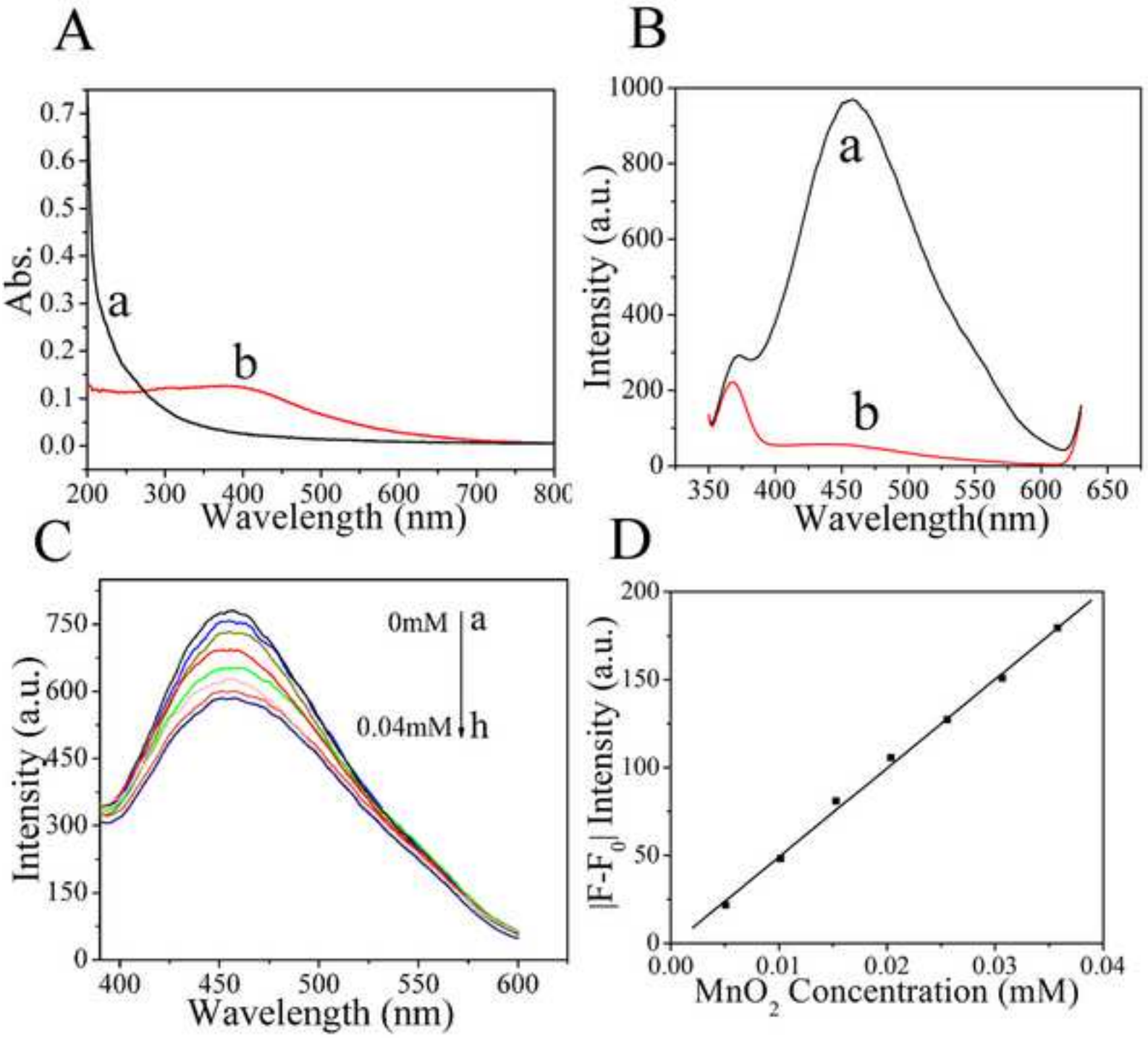
A
Abs.
a
b
Wavelength (nm)
B
Intensity (a.u.)
a
b
Wavelength(nm)
C
Intensity (a.u.)
0mM
a
0.04mM
h
Wavelength (nm)
D
|F-F0| Intensity (a.u.)
MnO2 Concentration (mM)

Figure 3

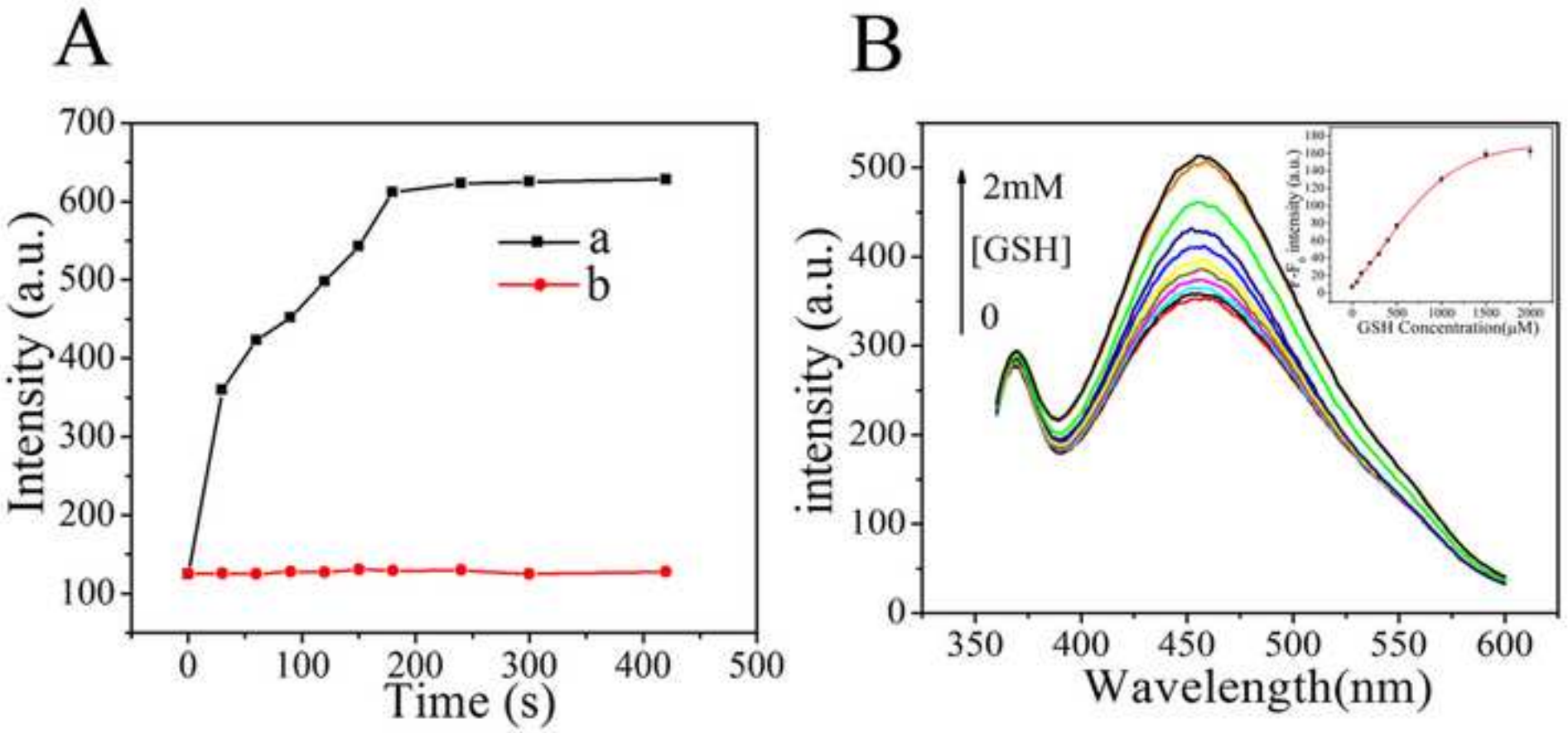
A
Intensity (a.u.)
Time (s)
a
b
B
intensity (a.u.)
Wavelength(nm)
2mM
[GSH]
0
GSH Concentration(μM)

Figure 4

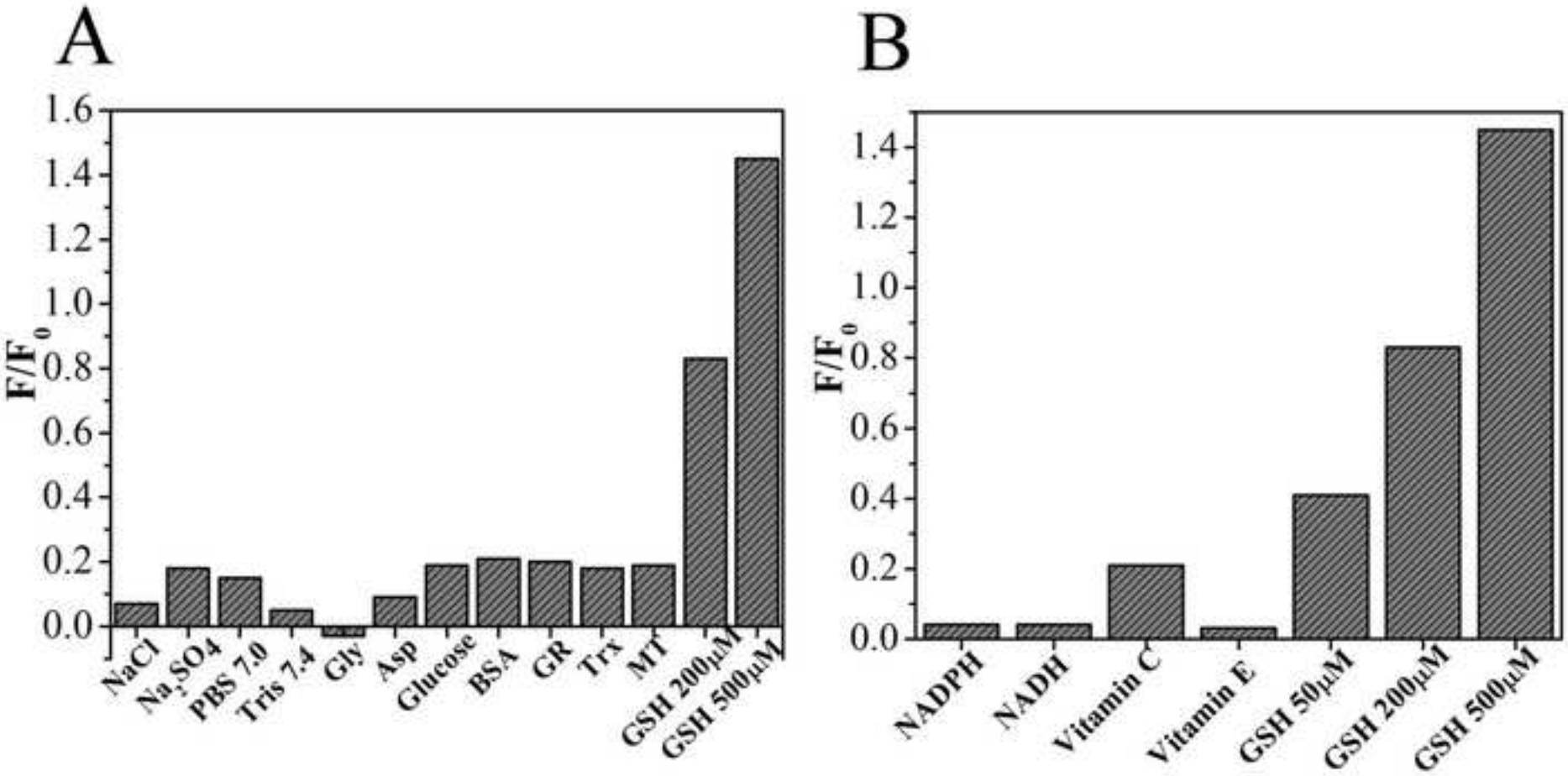
A
F/F0
1.6
1.4
1.2
1.0
0.8
0.6
0.4
0.2
0.0
NaCl
Na2SO4
PBS 7.0
Tris 7.4
Gly
Asp
Glucose
BSA
GR
Trx
MT
GSH 200μM
GSH 500μM
B
F/F0
1.4
1.2
1.0
0.8
0.6
0.4
0.2
0.0
NADPH
NADH
Vitamin C
Vitamin E
GSH 50μM
GSH 200μM
GSH 500μM